

## BRAKING PROCESS INFLUENCE ON VERTICAL LOAD OF RAILWAY VEHICLES

<sup>1-3</sup>. University POLITEHNICA of Bucharest, Faculty of Transports, Department of Railway Rolling Stock, ROMANIA

**Abstract:** The paper investigates the effects of pitch phenomenon during railway vehicles braking process. The variation of vertical loads on bogies and axles are presented for the case of emergency braking, analysing also the influence of mechanical wheel slide prevention devices intervention. In simulations, experimentally acquired data of the air pressure evolution in the brake cylinders are used. The simulations results are presented and discussed. The effects on braking process are enhanced, including the case of poor wheel-rail adhesion. Conclusions regarding the pitch effects and operational consequences of mechanical wheel slide prevention devices actuation during braking actions are formulated.

**Keywords:** railway vehicle, pitch, braking, vertical loads, wheel slide prevention devices

### INTRODUCTION

The main target of the present study is to evaluate the evolution of axle vertical load variation determined by the pitch phenomena during braking actions, enhancing the effects of the action of wheel slide prevention devices that occur in the case of poor adhesion.

It is known that pitch phenomenon determines supplementary vertical loadings / unloadings on bogies and axles, modifying accordingly the adhesion forces. Given that in the case of railway vehicles the wheel-rail adhesion is essential for the starting tractive effort and critical in braking process, limiting both traction and braking capacities, concerns about the consequent effects of pitch phenomena are legitimate.

An extensive study concerning the pitch of locomotives was conducted by dr. G. Borgeaud, published in 1967 in the Bulletin of L'Al du Congrès des Chemins de Fer [1]. In his paper, the author presents theoretical aspects as well as examples of calculations of the vertical load variations for different types of locomotives and axle drive action modes. Regarding the specific problems of braking, comprehensive experimental and theoretical studies were performed regarding wheel-rail adhesion, pitch phenomena and its effects on braking process; the safety of traffic was also analysed [2, 3]. Researches on the pitch phenomenon on railway vehicles during braking actions were also performed by C.Cole [4], McClanachan [5], Burada [6], Cruceanu [7] Crăciun [8] and others.

Under the action of inertial forces to which the rail vehicle is subjected during braking, variations of vertical loads occur on the bogie and axle spindles, exerting the suspension elements, affecting the comfort and also the integrity and safety of passengers and freight.

In the present paper, based on a classical model of a passenger railway vehicle on bogies with two suspension levels, the vertical load variations during braking generated by pitch are presented. For an accurate determination of braking forces, essential for the development of the studied phenomenon, experimental values of the

brake cylinder air pressure evolution, in different operational-like cases, were performed on a computerised testing stand. A simulation program was used for evaluation of pitch effects during emergency braking actions, originally taking into account repeated actuations of mechanical wheel slide prevention devices. Results are discussed and analysed and the main conclusions are outlined.

### THEORETICAL BASES

During braking, the vehicle components are subject to supplementary loads due to inertia forces and to forces developed in the brake rigging. When a braking action is performed, inertia forces  $I_c$  and  $I_b$  appear at the level of vehicle body and, respectively, at the level of the sprung part of the bogies – see Figure 1 [7, 9, 10].

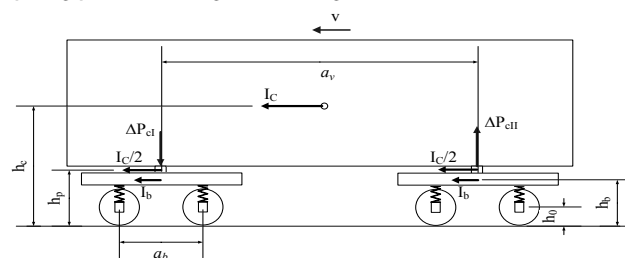


Figure 1. Forces acting on vehicle during braking

The body force of inertia  $I_c$  is transmitted evenly to bogies through the two links (pivots) and it is of the form:

$$I_c = m_c \cdot \ddot{x} \quad (1)$$

where  $m_c$  is the mass of vehicle body, and  $\ddot{x}$  is deceleration that develops during the brake action.

Because of the fact that this force can be considered to act in the centre of mass of the vehicle body, it produces a force couple (torque) which rotates the vehicle body about y axis, which is given by the following formula:

$$C_{yc} = m_c \cdot \ddot{x} \cdot (h_c - h_p) \quad (2)$$

where  $h_c$  is the height of the centre of mass of the vehicle body and  $h_p$  is the height of the connection point between the bogie and the vehicle body.

The pitch angle of the body caused by the action of the torque  $C_{yc}$  is [9]:

$$\varphi_{yc} = \frac{C_{yc}}{K_{xc}} \quad (3)$$

where  $K_{xc}$  is the body suspension longitudinal angular stiffness, given by:

$$K_{xc} = \sum_{i=1}^2 \sum_{j=1}^2 k_{cij} \cdot (x_{cij} - x_{c0})^2 \quad (4)$$

In eq. (4),  $x_{c0}$  is the  $x$ -coordinate of the centre of motion of the vehicle body;  $x_{cij}$  and  $k_{cij}$  are, respectively, the  $x$ -coordinates and the stiffness of the bogie-body suspension points.

Substituting equations (4) and (2) in equation (3), it becomes:

$$\varphi_{yc} = \frac{m_c \cdot \ddot{x} \cdot (h_c - h_p)}{\sum_{i=1}^2 \sum_{j=1}^2 k_{cij} \cdot (x_{cij} - x_{c0})^2} \quad (5)$$

For a railway vehicle equipped with two-axle bogies, characterized by elastic and geometric symmetry, we considered:

$$k_c = k_{cij}, i=1,2, j=1,2$$

$$x_{c11} = x_{c12} = x_{c1}, x_{c21} = x_{c22} = x_{c2}$$

The variation of the vertical loads introduced, by rotating the box, which appears in the box - bogie connection points are:

$$\begin{aligned} \Delta P_{cl} &= -2k_c (x_{c1} - x_{c0}) \varphi_{yc} \\ \Delta P_{cll} &= 2k_c (x_{c2} - x_{c0}) \varphi_{yc} \end{aligned} \quad (6)$$

for:  $x_{c0} = \frac{a_v}{2}$ ,  $x_{c11} = x_{c12} = 0$ ,  $x_{c21} = x_{c22} = a_v$ ,

where  $a_v$  is the vehicle wheelbase, the load variations in the bogie - box connection points can be written:

$$\Delta P_{cl} = -\Delta P_{cll} = m_c \cdot \ddot{x} \frac{(h_c - h_p)}{a_v} \quad (7)$$

It can be observed that the first bogie in the direction of displacement is loaded, while the second one is unloaded.

On the bogie frame, there appears a rotation torque due to inertial forces, which develop at the level of the vehicle body and at the level of the sprung part of the bogie:

$$C_{yb} = m_b \cdot \ddot{x} \cdot (h_b - h_0) + \frac{1}{2} m_c \ddot{x} \cdot (h_p - h_0) \quad (8)$$

where  $I_b = m_b \cdot \ddot{x}$  is the force of inertia of the bogie sprung part ( $m_b$  - mass of the sprung part of the bogie),  $h_b$  is the height of the centre of mass of the bogie and  $h_0$  is the height of the centre of the axle.

The pitch angle of the bogie frame caused by the action of the torque  $C_{yb}$  is given by:

$$\varphi_{yb} = -\frac{C_{yb}}{K_{xb}} \quad (9)$$

where  $K_{xb}$  is the bogie suspension longitudinal angular stiffness, which, in the case of a bogie with two axles, is given by:

$$K_{xc} = \sum_{i=1}^2 \sum_{j=1}^2 k_{bij} \cdot (x_{bij} - x_{b0})^2 \quad (10)$$

In previous relationship,  $x_{b0}$  is the  $x$ -coordinate of the centre of motion of the bogie;  $x_{bij}$  and  $k_{bij}$  are, respectively, the  $x$ -coordinates and the suspension stiffness corresponding to each axle journal.

Substituting the relations (8) and (10) in (9), it becomes:

$$\varphi_{yb} = \frac{m_b \cdot \ddot{x} \cdot (h_b - h_0) + \frac{1}{2} m_c \ddot{x} \cdot (h_p - h_0)}{\sum_{i=1}^2 \sum_{j=1}^2 k_{bij} \cdot (x_{bij} - x_{b0})^2} \quad (11)$$

As a result of the action of torque  $C_{yb}$  and of load variations  $\Delta P_{cl}$  and  $\Delta P_{cll}$ , on each bogie, a vertical load variation occurs on each axle journal.

The vertical load variation can be written [6, 7, 9]:

$$\Delta P_{ij} = k_{ij} \cdot [\pm f_z + (x_{bij} - x_{b0}) \cdot \varphi_{yb}] \quad (12)$$

where  $f_z$  is the vertical deflection of the axle suspension caused by load variations  $\Delta P_{cl}$  and  $\Delta P_{cll}$  which is equal and of opposite sign for the two bogies – see equation (7).

Assuming elastic and geometric symmetry of the bogies:

$$x_{b11} = x_{b12} = x_{b1} = 0, x_{b21} = x_{b22} = x_{b2} = a_b$$

$$x_{b31} = x_{b32} = x_{b3} = 0, x_{b41} = x_{b42} = x_{b4} = a_b$$

$$x_{b0} = \frac{a_b}{2}, k_{bij} = k_b, i=1,2,3,4; j=1,2;$$

where  $a_b$  is the bogie wheelbase, then, the vertical deflection of axle suspension can be written:

$$f_z = \frac{\Delta P_{cl}}{4k_b} = -\frac{\Delta P_{cll}}{4k_b} \quad (13)$$

and the supplementary vertical loads on axle journals can be written as:

$$\Delta P_{11} = \Delta P_{12} = k_b \cdot [f_z + (x_{b1} - x_{b0}) \cdot \varphi_{yb}] \quad (14)$$

$$\Delta P_{21} = \Delta P_{22} = k_b \cdot [f_z + (x_{b1} - x_{b0}) \cdot \varphi_{yb}]$$

for the first bogie, and

$$\Delta P_{31} = \Delta P_{32} = k_b \cdot [-f_z + (x_{b2} - x_{b0}) \cdot \varphi_{yb}]$$

$$\Delta P_{41} = \Delta P_{42} = k_b \cdot [-f_z + (x_{b2} - x_{b0}) \cdot \varphi_{yb}] \quad (15)$$

for the second bogie.

### THE BRAKE CYLINDER AIR PRESSURE DETERMINATION

Experiments to determine the brake cylinder air pressure evolution were performed on the passenger vehicle brake system stand in the laboratories of the Railway Vehicles Department of the Faculty of Transport, in University POLITEHNICA of Bucharest.

The dedicated stand is equipped with the bogie brake equipment used in operation for passenger rail vehicles. The air distributor is KE-type and the brake cylinder has 305 mm in diameter. There is a mechanical M2-type of wheel slide protection device on each of the two axles of the bogie of the stand. An air pressure transducer takes the pressure evolution in brake cylinder during the braking actions. The sample rate is 0.02 s and acquired data are processed and stored on a dedicated computer.

The elements of interest in these determinations were the evolutions of brake cylinder air pressure during emergency braking actions, for the cases of normal and poor wheel-rail adhesion. The second

situation was simulated by repeated actuations of the wheel slide protection device.

The interest regarding the effects of such equipment actuation is justified by the fact that the action of mechanical wheel slide protection devices is generally exerted on all the braked axles of the vehicle. More than that, there are induced in the brake cylinders large air pressure variations, having a high rate of decrease, respectively increase after adhesion regaining [7].

Samples of the determined pressure evolutions in the braking cylinder are presented in Figure 2 – 3 corresponding to emergency braking actions.

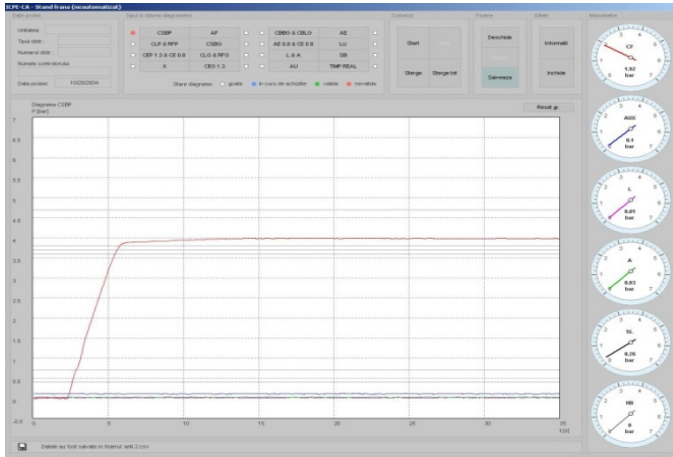


Figure 2. The evolution of pressure in the brake cylinder for the emergency brake action

Figure 3 emphasises the large and rapid air pressure variations in the brake cylinder determined by the repeated actuation of the mechanical wheel slide protection device during the first 10 s of the same braking action.

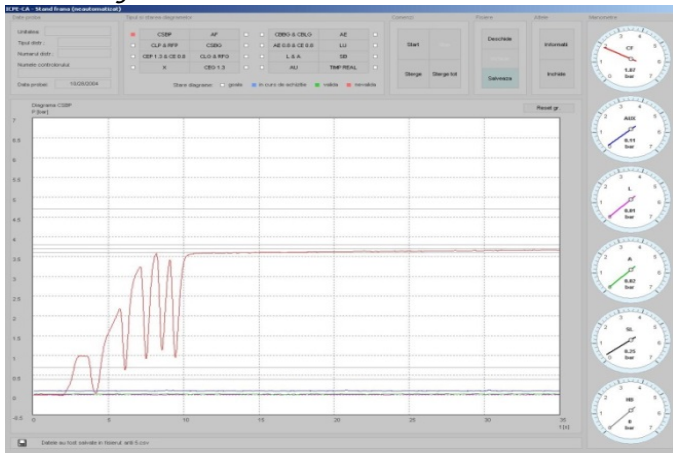


Figure 3. The evolution of the pressure in the brake cylinder with the actuations of wheel slide prevention devices at the beginning of the braking action

It is to expect that such evolution is going to have important influences on the instantaneous deceleration, hence on the pitch effects on the vehicle.

**SIMULATIONS ASSUMPTIONS AND DATA**

According to the main target of the present study and given the multiple factors influencing the development of pitch process during braking regime, a major preoccupation was to identify and eliminate,

as much as possible, any aspect potentially disturbing the direct influence of pressure evolution in brake cylinders experimentally determined.

Hence, certain constraints and simplifying hypotheses were assumed. Regarding the braking forces, their evolutions have relevant impact on the studied problem and, depending on the main braking system of the vehicle, can be determined [11]:

» for the case of disc brake equipped vehicle having individual self-adjusting brake rigging:

$$F_{b,i} = \left[ \frac{\pi \cdot d_{bc}^2}{4} \cdot p_{bc,i} - (F_R + R_{sa}) \right] \cdot i_t \cdot n_{bc} \cdot \frac{2 \cdot r_m}{D_o} \cdot \mu_d \cdot \eta_{br} \quad (16)$$

where:  $d_{bc}$  is the brake cylinder diameter,  $p_{bc,i}$  the instantaneous relative air pressure in the brake cylinder,  $F_R$  and  $R_{sa}$  the resistance forces due to the brake cylinders back spring and to the self-adjusting mechanism incorporated in the piston rod respectively,  $D_o$  the wheel diameter and  $r_m$  the medium friction radius. The dimensionless terms are:  $i_t$  the brake rigging amplification ratio,  $n_{bc}$  the number of brake cylinders of the vehicle,  $\mu_d$  the friction coefficient between brake pads and disc and  $\eta_{br}$  the mechanical efficiency of the brake rigging.

» for the case of cast iron shoe brake, with symmetrical brake rigging and self-adjusting mechanism on the main brake bar:

$$F_{b,i} = \left[ \left( \frac{\pi \cdot d_{bc}^2}{4} \cdot p_{bc,i} - F_R \right) \cdot i_c - R_{sa} \right] \cdot i_l \cdot n_{\Delta} \cdot n_{bc} \cdot \mu_s(P_s, V_i) \cdot \eta_{br} \quad (17)$$

The dimensionless terms are:  $i_c$  the central brake rigging,  $i_l$  the amplification ratio of the brake rigging's vertical levers,  $n_{\Delta}$  the number of triangular axles and  $\mu_s$  the friction coefficient between brake shoes and wheel tread which depends on the clamping force on each brake shoe  $P_s$  [kN] and on instantaneous running speed  $V_i$  [km/h].

Assuming that certain terms and factors representing constructive and functional characteristics are constant for the same vehicle during braking actions, one may be put in evidence that during the filling time the brake force for the brake disc is directly depending only on the instantaneous relative air pressure in the brake cylinder  $F_{b,i} = f(p_{bc,i})$ , while in the case of shoe brake, the dependence is more sophisticated due to the friction coefficient between brake shoes and wheel tread  $F_{b,i} = f(p_{bc,i}, \mu_s(P_s, V_i))$ .

Hence, a passenger coach equipped with brake discs was considered in simulations. It is to notice that in operation, exploitable braking forces develop only after reaching an approx. 0.4 bar pressure within the brake cylinder [12]. So, taking into account the adhesion influence and the experimentally determined data referring to the evolution in time of the air pressure in the braking cylinder  $p_{bc}(t)$ , the instantaneous braking forces during the process can be evaluated [13]:

$$F_b(t) = \begin{cases} 0 & \text{if } p_{bc}(t) < 0.4 \text{ bar} \\ p_{bc}(t) \cdot \mu_a \cdot m_v \cdot g & \text{if } p_{bc}(t) > 0.4 \text{ bar} \\ p_{bc,max} & \end{cases} \quad (18)$$



In eq. (18),  $\mu_a$  is denoting the wheel-rail adhesion coefficient,  $m_v = m_c + 2 \cdot (m_b + m_{nb})$  the mass of the vehicle,  $m_{nb}$  the unsuspended mass of the bogie,  $g$  the gravitational acceleration and  $p_{bc,max}$  the maximum air pressure experimentally determined for emergency braking in the cylinder.

Other relevant constraints and simplifying hypotheses are summed up as follows:

- » the vehicle is submitted to emergency braking, determining maximum possible deceleration;
- » mechanical wheel slide protection devices are considered because generate maximum possible deceleration variations during braking action;
- » the case of uniform distribution of the load per bogie and per wheel is adopted;
- » identical constructive and elastic characteristics of the elements of each suspension level;
- » the track is considered to have no curves or slopes, so only the main resistances were taken in account;
- » track irregularities are neglected.

Simulations were performed for an individual passenger coach and the main parameters are: mass of the vehicle  $m_v = 47$  t, mass of the sprung part of the bogie  $m_b = 5900$  kg, the height of the centre of mass for vehicle body  $h_c = 1.696$  m, the height of centre of mass of the bogie  $h_b = 0.608$  m, the elevation of the connection point between vehicle body and bogie  $h_p = 0.985$  m, the elevation of the axle spindles  $h_0 = 0.460$  m, the wheelbase of the vehicle  $a_v = 19$  m, the wheelbase of the bogie  $a_b = 2.560$  m, stiffness of the point of suspension of the box  $k_c = 5 \cdot 10^5$  N/m, stiffness of the point of suspension of the axle  $k_b = 6.45 \cdot 10^5$  N/m.

The initial velocity of the vehicle is considered 140 km/h and, for the maximum braking force value, the adhesion coefficient  $\mu_a = 0.1$  was taken into account.

The integration of the motion equation and numerical simulations were performed in Matlab using the solver ode45.

The main output parameters obtained with the simulation program are the time-histories evolutions of decelerations, vertical load variations on each bogie and axle spindles respectively, velocity and braking distance.

**NUMERICAL APPLICATION**

Simulations based on the previous presented data were performed for 20 s of emergency braking process. The main results of the numerical applications results for the cases of emergency braking action are presented in Figure 4... 8 in normal adhesion conditions and in Figure 9... with the actuations of the wheel slide prevention devices.

In the first case, the deceleration time history (see Figure 4) highlights first a small value at the beginning of the action, while only main resistant forces are implied and then the increase up to the maximal value of 1.0447 m/s<sup>2</sup>, corresponding to the maximum air pressure in the brake cylinders, followed by a slightly decrease determined by the

evolution of resistances recess while the vehicle is slowing down during the braking action.

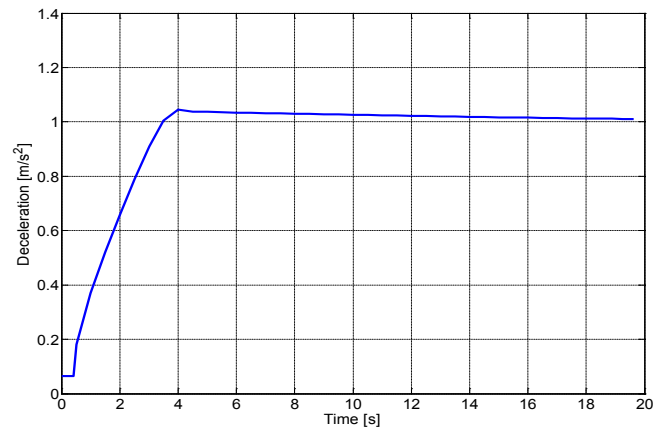


Figure 4. Deceleration in emergency braking action (normal adhesion conditions).

During the defined time duration, the brake distance reaches the value of 605 m and the vehicle's speed decreases from the initial value of 140 km/h to 72, 64 km/h (Figure 5).

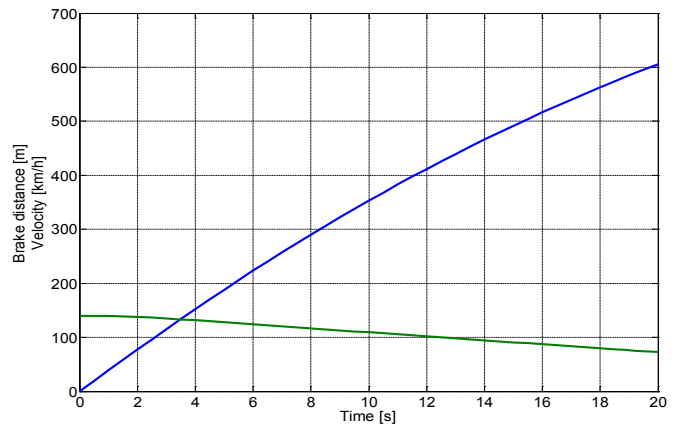


Figure 5. Brake distance and velocity during first 20 s of emergency braking action (normal adhesion conditions).

According to the deceleration evolution, the resultant vertical load variations ( $P_j$ ) on bogies and on each axle ( $P_{11} \dots P_{42}$ ) are presented in Figure 6, respectively 7. For identification, the number indexes of forces are in respect to the displacement direction. When the case, the second number index refer to the left side (odd numbers) and right side (even numbers) considering the vehicle's sense of motion.

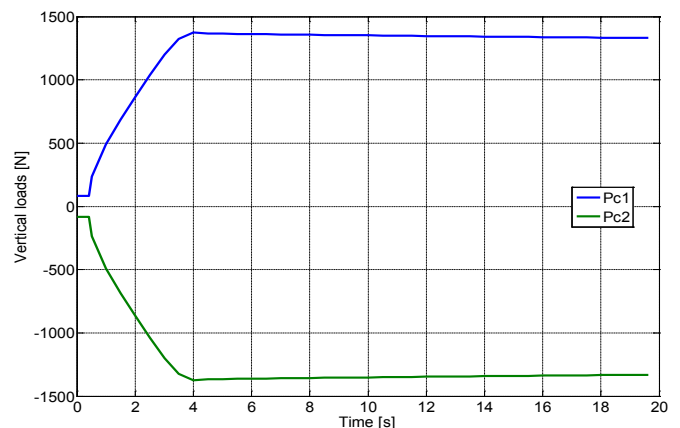


Figure 6. Variations of loads on the bogies of the vehicle (braking action in normal adhesion conditions).

As expected, the load variations are dependent of the deceleration evolution. The first bogie (towards the direction of movement) is supplementary charged, while the vertical load of the second one is correspondingly decreased (see Figure 7). Regarding the axles (see Figure 8), the results indicates supplementary loadings of the first and third axle, while the most unloaded are the second and the fourth, respectively.

This aspect deals with experiments highlighting a higher tendency of the fourth and second wheelsets of blocking during braking actions, as effect of vertical load decrease due to the vehicle's pitch [8, 14...16].

Interesting results were obtained in the case of occurrence of actuations of wheel slide prevention devices during the braking action (see Figure 9... 11).

The effects on braking process are presented in Figure 9: during the first 20 s, the braking distance is 36 meters longer than in the previous case (641 m) and the velocity decreases to the value of 81,6 km/h (about 10 km/h higher than in the first case). These aspects indicate the decrease of braking capacity.

The determined vertical load variations ( $P_c$ ) on bogies and on each axle ( $P_{11} \dots P_{42}$ ) are presented in Figure 10, respectively 11. Basically, the general pitch effects are the same, determining supplementary loadings on the first bogie and on the first and third axle of the vehicle and correspondent decreases on the others. Still, important variations are revealed, load variation evolutions following the decelerations modifications during braking actions generated by the repeated actuation of wheel slide prevention devices.

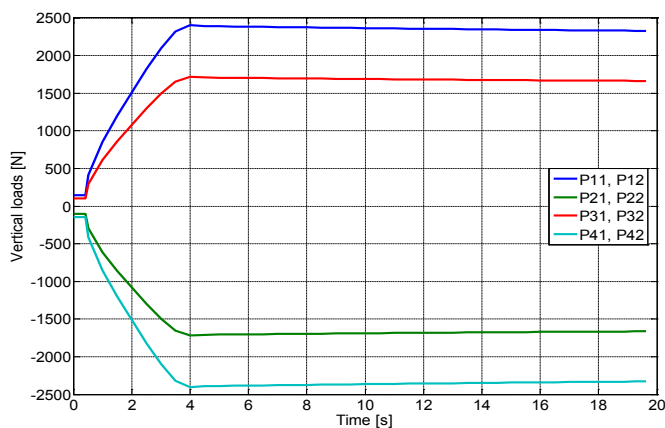


Figure 7. Variations of loads on the axle spindles (braking action in normal adhesion conditions).

In the second studied case, the deceleration evolution (see Figure 8) evidenciates important variations according to the braking forces modifications generated by the actions of the wheel slide prevention devices (see brake cylinder pressure time history in Figure 3). The deceleration increases with the increase of brake cylinders air pressure and correspondently falls when the wheel slide prevention device is actuated, generating a rapid decrease in pressure. The successive actuations conduct to high variations of the deceleration, the maximum instantaneous value reaching  $1,086 \text{ m/s}^2$ , increasing by 4 % as compared to the previous situation.

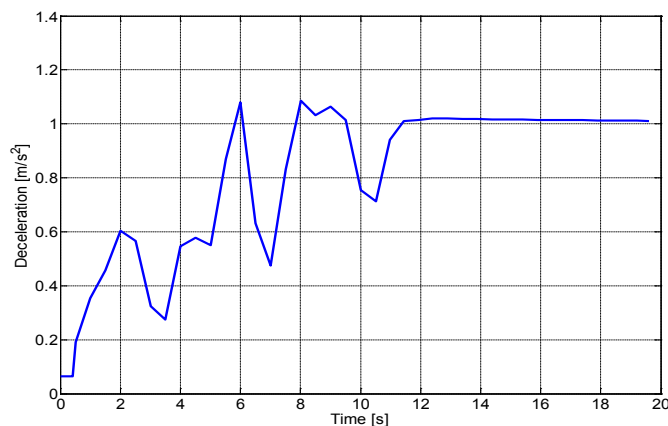


Figure 8. Deceleration during first 20 s of emergency braking action with actuation of wheel slide prevention devices.

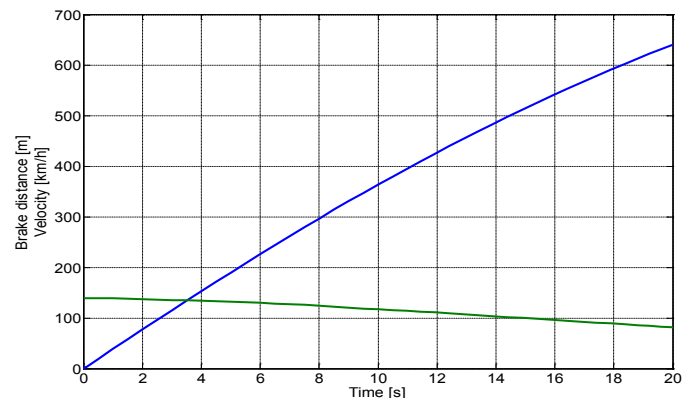


Figure 9. Brake distance and vehicle velocity with wheel slide prevention devices actuation.

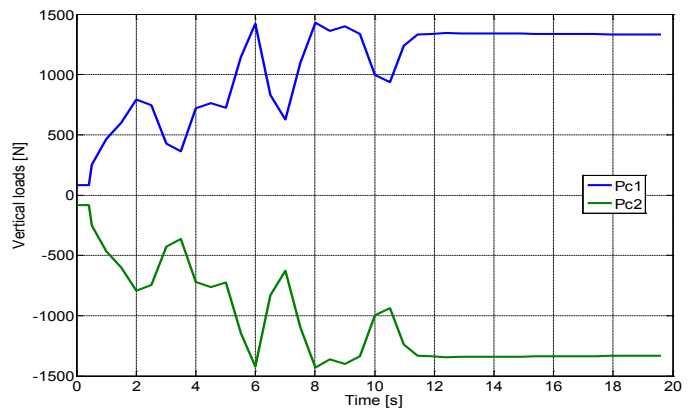


Figure 10. Variations of loads on the axle spindles (braking action in normal adhesion conditions)

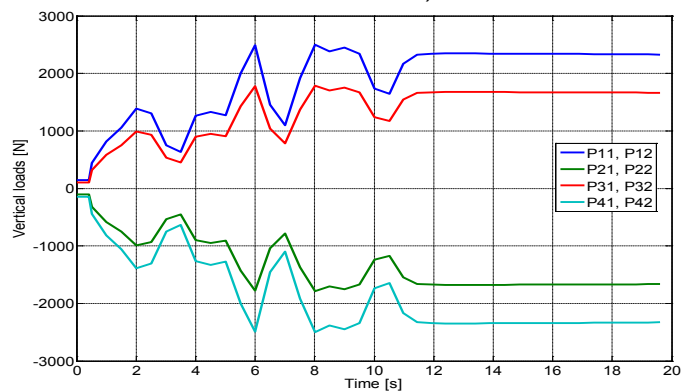


Figure 11. Loads variations in the axle spindles when the wheel slide prevention devices come into action

Regarding the braking process in the case of altered adhesion, the deceleration decrease during the actions of wheel slide prevention devices generates an instantaneous increase of vertical load on the axles, which combined with the important drop of braking force, accelerates the process of the initially brake cylinder air pressure regain. If the length of the low adhesion track is short, the rapid recovery of pressure minimises the brake power losses. On the contrary, if the length of the poor adhesion zone is important, in operation it is to expect repeated actuations of mechanical wheel slide prevention devices, almost in a periodically pulsating process. The average braking force may have high decrease, eventually accentuated by the rapid use of the compressed air from the auxiliary reservoir of the vehicle, affecting the safety of the traffic.

### CONCLUSIONS

The main influences of the actuation of mechanical wheel slide prevention devices upon the load variations during braking process can be summarised as follows:

- » the vertical load on axles is affected due to the vehicles' pitch during braking actions, with potential impairment of traffic safety;
- » simulations confirm a higher tendency of the fourth and second wheel sets in blocking during braking actions, as effect of vertical load decrease due to the vehicle's pitch;
- » the load variations evolution is determined by the deceleration variations generated by the air pressure evolution in the brake cylinders of the vehicle;
- » the effect of wheel slide prevention devices action on vertical load of the axles, combined with important drop of braking force, accelerates the process of the commanded brake force regain;
- » regarding the safety of the braking process, repeated wheel slide prevention devices actuations increase the braking distance and diminish the velocity decrease rate;
- » for short low-adhesion zones, the rapid recovery of pressure minimises the brake power losses;
- » on long poor adhesion zones the mechanical wheel slide prevention devices can affect the safety of the traffic, especially in the case of relatively high velocities and emergency braking actions. In such cases, electronic wheel slide prevention devices are required.

### References

- [1.] Borgeaud G., L'effet du cabrage sur les modifications des charges d'essieu d'une locomotive à deux bogies et moyens d'y remédier, Bulletin de L'A.I. du Congrès des Chemins de Fer, pp.691-739, novembre 1967.
- [2.] O.R.E., Question B 164. Adhérence en freinage et anti-enrayage. Rapport No. 1: Synthèse des connaissances actuelles sur l'adhérence en freinage, Utrecht, sept., 1985.
- [3.] O.R.E., Question B 164. Adhérence en freinage et anti-enrayage. Rapport No. 2: Lois fondamentales de l'adhérence en freinage, Utrecht, avril 1990.

- [4.] Cole, C., Longitudinal train dynamics, chapter 9 in Handbook of Railway Vehicle Dynamics, edited by Simon Iwnicki, Ed. Taylor & Francis Grup, ISBN 978-0-8493-3321-7, pp. 239-277, 2006.
- [5.] McClanachan, M., Cole, C., Roach, D., Scown, B., An Investigation of the Effect of Bogie and Wagon Pitch Associated with Longitudinal Train Dynamics, The Dynamics of Vehicles on Roads and on Tracks-Vehicle System Dynamics Supplement 33, Swets & Zeitlinger, Amsterdam, pp. 374–385, 1999.
- [6.] Burada, C., Buga, M., Crăneanu, C., Elemente și structuri portante ale vehiculelor feroviare, Ed. Tehnică, București, 1980.
- [7.] Cruceanu, C., Frâne pentru vehicule feroviare, ed.a III-a, Ed. MatrixRom, București, 2009.
- [8.] Crăciun C., Contribution on the dynamic phenomena which occur during train braking, Doctoral Thesis, University POLITEHNICA of Bucharest, Romania, 2014.
- [9.] Popa, G., Țăruș, B., Structuri portante pentru vehicule feroviare, Ed. MatrixRom, ISBN 973-685-967-3, București, 2005.
- [10.] Zeng, J., Luo, R., Non-linear Analysis of Disc Brake-Induced Vibration for Railway Vehicles, Proceedings of Institution of Mechanical Engineers, Part F: Journal of Rail and Rapid Transit, DOI: 10.1243/09544097JRR307, pp.48-56, 2011.
- [11.] Cruceanu, C., Train braking (Chapter 2) in Reliability and Safety in Railway, InTech, Editor Xavier Perpinia, p. 29-74, 2012.
- [12.] UIC leaflet 540: Brakes - Air Brakes for freight trains and passenger trains, 5th edition, Nov. 2006
- [13.] Cruceanu, C., Crăciun, C., Influence of Application Time Regulated Limits on Longitudinal Dynamic Forces in Passenger Short Trains during Braking Process, Mathematical Applications in Modern Science, Proc. of the 19th International Conference on Applied Mathematics, Istanbul, Dec. 15-17, pp. 136-145, 2014.
- [14.] Boiteux, M., Les antienrayeurs modernes. Principes constructifs. Essais par la S.N.C.F. de l'antienrayeur Faiveley AEF 83 P, R.G.C.F., 105e année, février 1986, pp. 73-81.
- [15.] Boiteux, M., Le problème de l'adhérence en freinage, R.G.C.F., 105e année, février 1986, pp. 59-72.
- [16.] Boiteux, M., Influence de la vitesse et de différents paramètres constructifs sur l'adhérence en freinage, R.G.C.F., 109e année, février 1990, pp. 31-38.

**ACTA Technica CORVINIENSIS**  
BULLETIN OF ENGINEERING

**ISSN:2067-3809**

copyright ©

University POLITEHNICA Timisoara, Faculty of Engineering Hunedoara,  
5, Revolutiei, 331128, Hunedoara, ROMANIA

<http://acta.fih.upt.ro>